ISSN 1063-7842, Technical Physics, 2015, Vol. 60, No. 10, pp. 1529–1534. © Pleiades Publishing, Ltd., 2015.
Original Russian Text © D.Ya. Sukhanov, K.V. Zav'yalova, 2015, published in Zhurnal Tekhnicheskoi Fiziki, 2015, Vol. 85, No. 10, pp. 115–120.

RADIOPHYSICS

3D Radio Tomography of Objects Hidden behind Dielectrically Inhomogeneous Shields

D. Ya. Sukhanov* and K. V. Zav'yalova
Tomsk National Research State University, pr. Lenina 36, Tomsk, 634050 Russia
**e-mail: sdy@mail.tsu.ru*
Received October 10, 2014

Abstract—A method for the reconstruction of 3D radio images of objects that are hidden behind a priori known dielectrically inhomogeneous shields is based on the results of multiposition ultrabroadband radio sounding. Direct and inverse problems are solved in the Kirchhoff approximation and the scalar approximation of single scattering. Numerical simulation and experimental study are performed at frequencies ranging from 4 to 14 GHz. It is demonstrated that distortions of reconstructed images of hidden objects can be eliminated with allowance for the diffraction by dielectric shields.

DOI: 10.1134/S106378421510028X

INTRODUCTION

3D radio tomography is employed in archaeology, geology, and the problems of building of roads and engineering objects. The highest spatial resolution of reconstructed images can be obtained using the technologies of synthesized aperture [1–5] and ultrabroadband signals. Several methods make it possible to reconstruct 3D radio images using ultrabroadband monostatic sounding in homogeneous media [3–5]. Note the solution for inhomogeneous media, in particular, sounding via a plane interface of media [6] and plane-layered media [7]. Such methods employ the location measurements of field on the surface above the volume under study using the single-scattering approximation and assumption on the homogeneity of background medium. In practice, the background medium is normally inhomogeneous with respect to electric properties and electric inhomogeneities may have arbitrary shapes. Background inhomogeneities lead to the distortions of the wave propagation trajectories that must be taken into account in the solution of the inverse problem of reconstruction of images of objects under study. For a plane-layered medium, the transformations of fields in the layers can be taken into account in the spectrum of plane waves using multiplication by a phase factor [7]. When the sounding is performed via an irregular interface of media, the boundary effect can be taken into account in the phase-screen approximation [8]. However, even the solution of the direct problem of the wave propagation becomes nontrivial and necessitates several approximations if the background medium exhibits arbitrary shapes of boundaries between regions with different electric properties. The solution of the inverse problem is impossible in the absence of the solution to the direct problem. A few methods can be used to solve the direct and inverse problems of wave propagation in gradually inhomogeneous media [9, 10]. Note also solutions to the problems of diffraction by objects with the simplest geometrical configurations (e.g., sphere, wedge, cylinder [11], and cone) that can be used in practice in several particular scenarios.

In this work, we propose a method for the reconstruction of 3D images of scattering objects hidden in an inhomogeneous background medium with arbitrary interfaces between regions with different electric properties. We assume that the shapes of interfaces and electric properties of the fractions of medium are known.

1. MEASUREMENT SCHEME AND FORMULATION OF THE PROBLEM

We consider a scheme for the monostatic sounding with the frequency scanning in a relatively wide band (Fig. 1). The emitter and receiver that are close to each other form a transceiver unit that is shifted along the horizontal plane with a step that is less than one quarter of a wavelength. Omnidirectional receiving and transmitting antennas are employed. At each position of the transceiver unit, monochromatic signals are emitted and the field intensity in the receiving antenna is measured. The waves emitted by the transmitting antenna pass through a dielectrically inhomogeneous medium with different refractive indices in which refraction and diffraction take place. Then, the wave field is incident on the object under study and scattered. The field that is scattered by the object passes in the backward direction through the inhomogeneous medium and is incident on the receiving antenna. The

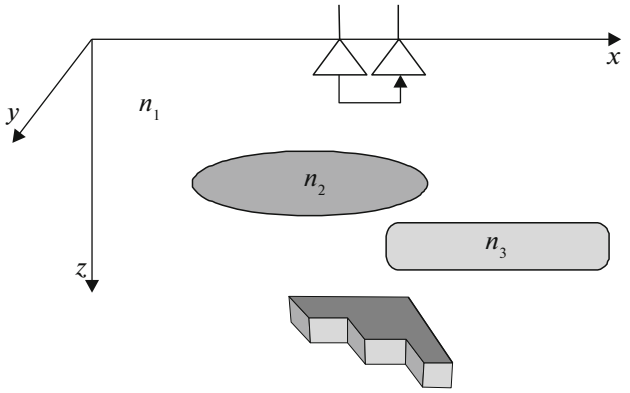

Fig. 1. Measurement scheme.

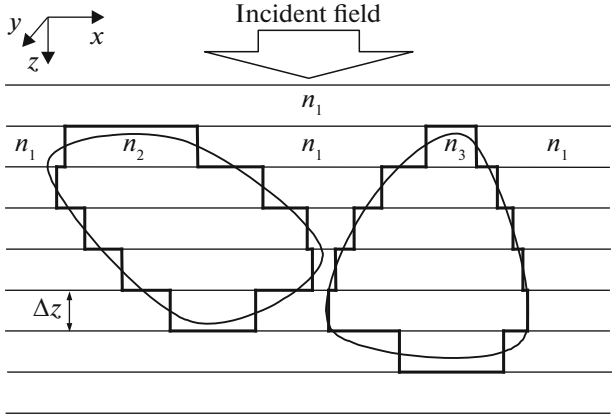

Fig. 2. Division of the inhomogeneous medium into thin layers.

interference of the field that is scattered by the inhomogeneities under study (object wave) and the field of the forward (reference) wave occurs in the antenna, and the intensity of the resulting field is measured. The phase information for the object wave is measured with an accuracy of $\pm\pi/2$ owing to the interference [3].

2. SOLUTION OF THE DIRECT PROBLEM

We determine the field of the object wave in the measurement region using the given distribution of the scattering inhomogeneities. For this purpose, we consider the propagation of radio waves through a dielectrically inhomogeneous medium at a single frequency. We divide the dielectrically inhomogeneous medium into thin horizontal layers with a thickness of $\Delta z \ll \lambda$. Using such layers, we approximate the shapes of dielectric inhomogeneities with the aid of vertical boundaries in each layer (Fig. 2). Thus, the dielectric inhomogeneity in each layer depends only on horizontal coordinates. We also assume that the set of the possible values of refractive index is countable and finite. Figure 2 presents a system with only three values of refractive index.

We perform the layer-by-layer calculation of the field in the medium, so that field $U(x, y, z + \Delta z)$ at the lower boundary of the layer at a depth of $z + \Delta z$ is calculated using field $U(x, y, z)$ at the upper boundary at a depth of z. We employ M values of refractive index and calculate the field at a depth of $z + \Delta z$ for M different homogeneous layers at depth z.

Using the expansion in spectrum of plane waves, we represent the field having passed through a homogeneous layer with refractive index n_m as [12]

$$U_m(x, y, z + \Delta z) = \int_{-\infty}^{\infty}\int_{-\infty}^{\infty} \widetilde{U}(k_x, k_y, z)\exp\left(ik_x x + ik_y y + ik_{mz}\Delta z\right)dk_x dk_y, \quad (1)$$

where $k_{mz} = \sqrt{(kn_m)^2 - k_x^2 - k_y^2}$ is the z component of the wave vector in the medium with refractive index n_m, m ranges from 1 to M,

$$\widetilde{U}(k_x, k_y, z) = \frac{1}{(2\pi)^2} \times \int_{-\infty}^{\infty}\int_{-\infty}^{\infty} U(x, y, z)\exp\left(-ik_x x - ik_y y\right)dxdy$$

is the spectrum of plane waves at the exit from the previous layer, and $U_m(x, y, z + \Delta z)$ is the field at the exit of the current layer if the medium therein is homogeneous and has refractive index n_m.

Then, we join M solutions $U_m(x, y, z + \Delta z)$ with allowance for the distribution of refractive index $n(x, y, z)$. The resulting field in the next layer is written as

$$U(x, y, z + \Delta z) = U_m(x, y, z + \Delta z), \quad \text{if } n(x, y, z) = n_m. \quad (2)$$

Using iterative procedure (2), we can calculate the field in the entire medium. However, we assume that the internal field of the layer does not propagate from one medium into another along the horizontal direction. The thinner the layers, the more accurate such an approximation. In addition, note that the above solution can be used for media with any countable number of refractive indices but an increase in the number of different refractive indices $n(x, y, z)$ causes an increase in the amount of computations. Note also that we disregard single and multiple reflections from the transitions between media of different types. Such reflections can be taken into account using reflection and transmission coefficients of plane waves in the plane-layered medium. Normally, the amplitudes of the waves that result from single and multiple reflection from dielectric inhomogeneities are less than the amplitude of the forward wave, so that the reflected waves can be disregarded. We consider variations in

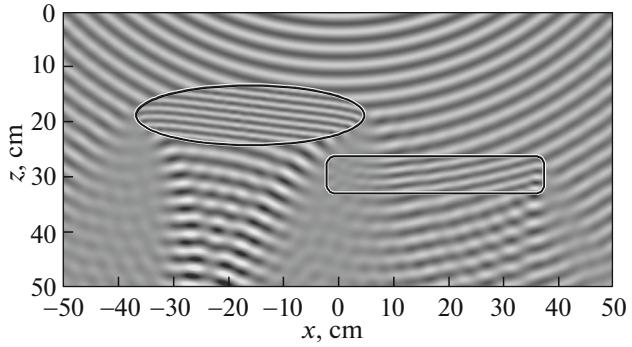

Fig. 3. Result of the numerical simulation of the field in the medium with three different refractive indices (the contour shows the region of the dielectric inhomogeneity).

phase rather than amplitude and, for simplicity, do not take into account transmission coefficients in expression (2).

With the aid of formula (2), we numerically simulate the medium with three different refractive indices: $n_1 = 1$, $n_2 = 1.5$, and $n_3 = 2$. We consider objects that are shown with contours in Fig. 3: the refractive indices of the background medium and elliptical and rectangular objects are 1, 1.5, and 2, respectively. In the numerical model, we use a frequency of 10 GHz. A source of spherical waves is located at an altitude of 50 cm above the system under study.

We observe refraction and diffraction and the generation of nonuniform waves in the presence of total reflection. We also observe the focusing of the wave field.

The field of the source having passed through dielectric inhomogeneities is incident on the scattering objects in the medium. Then, the field of the wave that propagates from the objects to the receiver through the same dielectric inhomogeneities emerges. The scattered waves that pass through the dielectric inhomogeneities are taken into account using formulas similar to formula (2) with changing of the direction of the vertical axis. However, significant amounts of computations are needed for the calculation of the incident and scattered fields for each position of the transceiver unit. To simplify the computations, we use the reciprocity theorem in accordance with which the field that passes from a single emitter to the scatterer coincides with the field that passes in the opposite direction. On the assumption that a source with the same intensity is located at the point of scattering (i.e., for the monostatic measurement scheme in which the emitter and receiver are located at the same point), we may change the scatterer by an equivalent source that emits at the doubled frequency. Such a substitution is possible, since the phase shifts related to the propagation of waves to the scatterer and in the opposite direction are equal to the phase shifts at the doubled frequency upon propagation from the scatterer to receiver. Thus, the field in the measurement region can be represented as the field of the in-phase sources that are located at the points of scatterers and emit at the doubled frequency.

3. SOLUTION OF THE INVERSE PROBLEM

To solve the inverse problem, we use the method of the backward field propagation. The inverse problem is solved in the inverse order with respect to the solution of the direct problem, so that the measured field is used to reconstruct the field distribution in the medium. Similarly to the solution of the direct problem, we consider the field in discrete layers with thickness Δz.

The backward-propagating field having passed through a homogeneous layer with refractive index n_m is represented using the expansion in the spectrum of plane waves:

$$W_m(x,y,z+\Delta z) = \int_{-\infty}^{\infty}\int_{-\infty}^{\infty} \widetilde{W}(k_x,k_y,z)\exp(ik_x x + ik_y y) \times\left[\exp\left(ik'_{mz}\Delta z\right)\right]^* dk_x dk_y, \quad (3)$$

where

$$\widetilde{W}(k_x,k_y,z) = \frac{1}{(2\pi)^2} \times \int_{-\infty}^{\infty}\int_{-\infty}^{\infty} W(x,y,z)\exp(-ik_x x - ik_y y)\,dxdy$$

is the spectrum of plane waves of the reconstructed field at the exit from the previous layer, $k'_{mz} = \sqrt{(2kn_m)^2 - k_x^2 - k_y^2}$ z-component of the wave vector of the field of equivalent sources at the doubled frequency in the medium with refractive index n_m, $W_m(x, y, z + \Delta z)$ is the reconstructed field at the exit from the current homogeneous layer with refractive index n_m, and $W(x, y, z)$ is the reconstructed field of the equivalent sources at the doubled frequency. Factor $\left[\exp\left(ik'_{mz}\Delta z\right)\right]^*$ in the integrand in expression (3) makes it possible to take into account the backward propagation of uniform waves but does not take into account the backward propagation of nonuniform waves to avoid the divergence of the solution in the presence of the noise of the measured field.

Then, we join M solutions $W_m(x, y, z + \Delta z)$ with allowance for the distribution of refractive index $n(x, y, z)$. The resulting field in the next layer is represented using the joining of solutions for different media:

$$W(x,y,z+\Delta z) = W_m(x,y,z+\Delta z), \quad \text{if } n(x,y,z) = n_m. \quad (4)$$

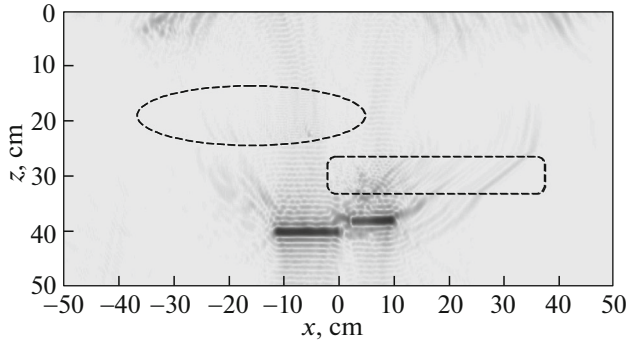

Fig. 4. Reconstructed image of scattering inhomogeneities upon monostatic sounding in a frequency band of 5–20 GHz.

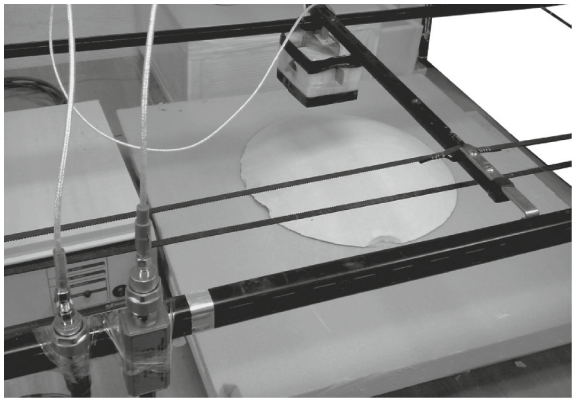

Fig. 5. Photograph of the experimental setup.

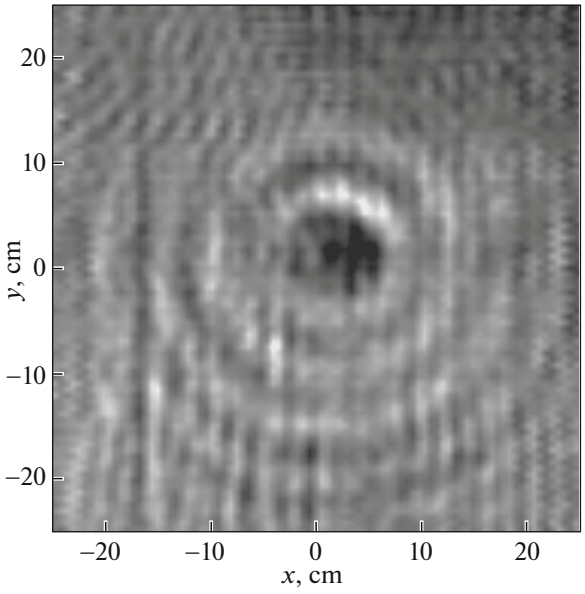

Fig. 6. Result of measurements at a frequency of 8 GHz.

Field $W(x, y, z = 0)$ is the field in the measurement region, which is used to reconstruct total distribution $W(x, y, z)$ with the aid of formulas (3) and (4). The total distribution is generated by equivalent sources with disregard of nonuniform waves.

To reconstruct the image of the object with the depth resolution, we need ultrabroadband measurements of the scattered field. Function $W(x, y, z, \omega)$ is the reconstructed field distribution at frequency ω that is calculated using formulas (3) and (4). This function is different at different frequencies but its phase at the position of the scattering object must be zero, since the object is considered as an equivalent in-phase source. Thus, the summation of functions $W(x, y, z, \omega)$ at different frequencies is the in-phase summation at the positions of scattering objects. At the remaining points, the summation is performed with arbitrary phases, so that the maximum is reached at the position of scatterer:

$$P(x, y, z) = \int_{\omega_{min}}^{\omega_{max}} W(x, y, z, \omega)\, d\omega. \qquad (5)$$

Here, $P(x, y, z)$ is the reconstructed image of the scattering objects, ω_{min} is the minimum frequency of the sounding signal, and ω_{max} is the maximum frequency of the sounding signal.

Figure 4 presents the result of the numerical simulation for the reconstruction of image of a test object that represents two segments with lengths of 12 and 8 cm for the measurements in a frequency band of 5–20 GHz. The measurement region (aperture) is 1 m, and the field is measured at an altitude of $z = 0$.

The reconstructed image contains artifacts, since the reconstruction of the distribution of nonuniform waves is not performed in formula (3). The resulting resolution with respect to distance (2 cm) corresponds to the theoretical estimation for the ultrabroadband sounding $c/\Delta f$, where c is the speed of light in the medium and $\Delta f = 15$ GHz is the bandwidth.

4. EXPERIMENTAL STUDY

Figure 5 shows the experimental setup that is used for the experimental study of the proposed method. A Micran R2M18/2 scalar circuit analyzer is employed to generate and measure signals. The device makes it possible to measure signal amplitudes at frequencies of up to 20 GHz. The transmitting and receiving antennas are placed in the transceiver unit that provides the forward (reference) signal from the transmitter to receiver. The signal of the transmitting antenna is incident on the scattering objects in the medium. The scattered signal is detected by the receiving antenna as an object signal, and the interference of the object and reference signals takes place. The interference makes it possible to reconstruct the cosine quadrature of the object signal. The frequency scan-

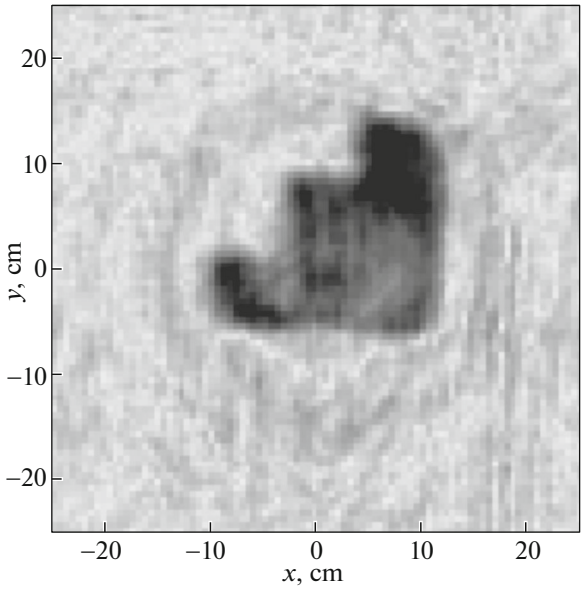

Fig. 7. Reconstructed image of object with disregard of the effect of the gypsum lens.

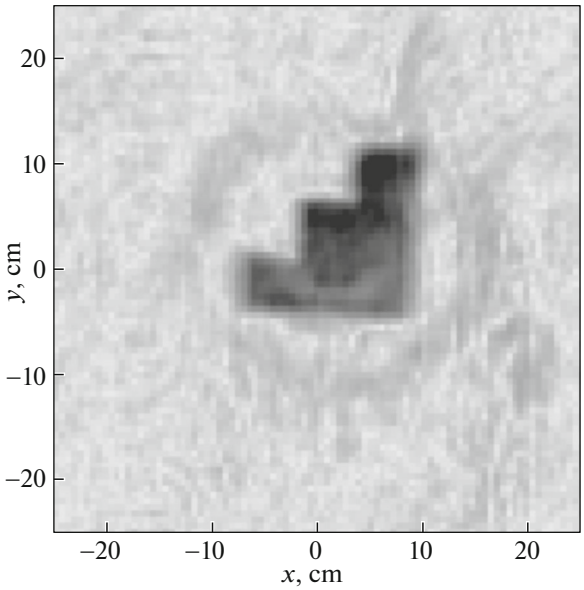

Fig. 8. Reconstructed image of object with allowance for the effect of the gypsum lens.

ning allows the ultrabroadband measurements. The sounding is performed in a frequency interval of 4–14 GHz. A gypsum convex lens with a diameter of 33.5 cm and an altitude of 6 cm serves as a dielectric shield in the experiments. The lens is placed at a distance of 12.5 cm from the sounding system. A step-shaped object with sizes of 15 × 15 cm and a step size of 5 cm is placed behind the lens at a distance of 8 cm. The transceiver unit moves along a region with sizes of 50 × 50 cm with a step of 5 mm.

The experiments yield a 3D data array of the quadratures of the object signal for each position of the transceiver unit at 512 frequencies ranging from 4 to 14 GHz. Figure 6 shows the result of the amplitude measurements for the interference of the fields of the reference and object signals at a frequency of 8 GHz.

The dominant signal is reflected from the lens. The signal of the object under study is almost undistinguishable, so that the processing is needed for the detection. The processing of the measured data is performed using the method of spatially matched filtering with disregard of the dielectric shield. Figure 7 presents the reconstructed image of the object. The image is distorted and seems to be magnified. The lens causes magnification of the image, since the object size in the image is about 20 cm whereas the real size is 15 cm.

Using formulas (3) and (5), which take into account the shape of the dielectric shield (gypsum lens) with a refractive index of 1.5, we reconstruct the image of the test object (Fig. 8). It is seen that the distortions are eliminated and the sizes correspond to the real sizes.

Note an increase in the signal-to-noise ratio due to the concentration of the energy of the desired signal in a single plane at the points where the object is located. The proposed processing makes it possible to identify the shape of the object.

CONCLUSIONS

We have proposed a method for the visualization of scattering inhomogeneities that are hidden behind dielectric shields with unknown shapes using the monostatic ultrabroadband multiposition sounding. For the experimental verification of the method, we have visualized objects hidden behind a gypsum lens. The proposed approaches can be employed in the problems of subsurface radars related to the detection and visualization of hidden objects, in particular, problems of archaeology and building of various structures, roads, and infrastructure.

REFERENCES

1. G. S. Kondratenkov and A. Yu. Frolov, *Radio Vision. Radar Systems for Remote Sensing of the Earth: Textbook for Institutions of Higher School,* Ed. by G. S. Kondratenkov (Radiotekhnika, Moscow, 2005).
2. V. P. Yakubov, S. E. Shipilov, D. Ya. Sukhanov, and A. V. Klokov, *Radiowave Tomography: Achievements and Perspectives,* Ed. by V. P. Yakubov (NTL, Tomsk, 2014).
3. V. P. Yakubov, K. G. Sklyarchik, R. V. Pinchuk, D. Ya. Sukhanov, A. N. Bulavinov, and A. D. Bevetskii, Izv. Vyssh. Uchebn. Zaved., Fiz. **51** (10), 63 (2008).
4. D. Ya. Sukhanov and K. V. Zav'yalova, Tech. Phys. **57** 819 (2012).

5. D. Ya. Sukhanov and K. V. Zav'yalova, Izv. Vyssh. Uchebn. Zaved., Fiz. **55** (9/2), 17 (2012).

6. V. P. Yakubov and D. Ya. Sukhanov, Izv. Vyssh. Uchebn. Zaved., Radiofiz. **50**, 329 (2007).

7. D. Ya. Sukhanov and K. V. Zav'yalova, Tech. Phys. **59**, 1854 (2014).

8. D. Sukhanov and K. Zavyalova, in *Proceedings of the 15th International Conference on Ground Penetrating Radar (GPR 2014), Brussels, Belgium, 2014,* pp. 691–695.

9. D. S. Bardashov and D. V. Losev, Izv. Vyssh. Uchebn. Zaved., Fiz. **56** (8/2), 32 (2013).

10. D. S. Bardashov and D. V. Losev, Izv. Vyssh. Uchebn. Zaved., Fiz. **56** (8/2), 177 (2013).

11. E. V. Shepilko, Izv. Vyssh. Uchebn. Zaved., Radiofiz. **45**, 26 (2002).

12. M. B. Vinogradova, O. V. Rudenko, and A. P. Sukhorukov, *Theory of Waves* (Nauka, Moscow, 1979).

Translated by A. Chikishev